Missile Impact Location Prediction Using Noisy Range Data

Matthew Hanson, Kevin Tibbetts, Ron Wohlers
Photon Research Associates, Inc. 1320 Center St.,
Suite 201, Newton, MA 02459
617-527-0054, matt@ktaadn.com

Jack D. Hart, Radian International
8501 N. Mopac Blvd., P.O. Box 201088
Austin, TX 78720-1088
512-419-5269, Jack_Hart@radian.com

Abstract-- Predicting the impact location of Theater Ballistic Missile (TBM) RV's has typically required tracking data from one or more traditional active and/or passive radar systems. When engine thrust terminates at booster engine cutoff (BECO), integration beyond burnout also requires an accurate state vector at the initiation of ballistic flight, and a reasonable estimate of the RV ballistic coefficient. The proposed algorithm requires no traditional radar data, but incorporates a single collector passive IR metric data set, and a slant range data set acquired via a PRA/KTAADN Monocular Passive Ranging (MPR) algorithm. The proposed study using IR metric and MPR data sets demonstrates the accuracy to which handoff state vectors (burnout to ballistic mode) must be known in order to achieve acceptable impact location accuracy's. The study results demonstrate that using the less accurate (but also less expensive than radar) single collector MPR and IR metric data sets provides sufficient accuracy to produce useful RV impact location predictions.

TABLE OF CONTENTS

1. INTRODUCTION

This report describes the theory and design of an algorithm for predicting the impact point of a missile based on the outputs of a single passive sensor obtained during the missile boost phase.

Theater ballistic missiles are a serious and growing threat in both major and brush fire conflicts. This threat is aggravated by their proliferation into developing and in some cases rogue nations. Significant improvement in theater missile defense (TMD) can be achieved by providing early detection, identification and tracking of TBM's during the boost phase, when the missiles are below the radar horizon of defensive radars.

Early detection and tracking of TBMs can lead to estimates of launch point and trajectory for:

- Timely vectoring of counter strikes against TBM launchers
- Prediction of cueing volumes for significantly reducing search volume and power requirements of defense radars
- The prediction of impact point for supplying advanced warning to potential impact areas.

The main focus of this paper is that of impact location and post-boost trajectory reconstruction. Determination of launch point, useful for belated detection above cloud decks, is expected to be covered in future work.

1.1 Need for Passive Ranging

Range to military targets is a central need of war operations. Ranging is carried out by a forward observer's trained eye, known landmarks, and optical range finders. Since 1940 radar has greatly advanced ranging performance over long distances in most weathers. Other emitting (active) means use acoustics and laser sources.

Radar, the premier ranging sensor, attracts immense counter measure (CM) efforts. Passive CMs, such as signature modification, vary from cheap chaff to costly stealth aircraft. Active CMs, including anti-radiation missiles (ARM) which home on radar emissions, are proliferating globally. Over 2000 AGM-45 Shrikes and AGM-88 HARMs were used in Operation Desert Storm [1]. All sides will increasingly use

0-7803-5846-5/00/$10.00 © 2000 IEEE

new ARMs, e.g. China's new "AWACS-killer missile" [2]. ARMs will considerably hamper air defense and surveillance radars. Radar life times may be shortened or, at the least, vital radars may be forced "off the air" at crucial moments.

Ranging in XXIst century battlefields that are populated with ARMs will be based on new technologies. One option advances radar electronic measures to cope with intense CM environments. A second seeks new ranging means. This paper discusses an approach for passive ranging to bright military targets by using atmospheric spectral properties. This approach uses monocular passive ranging (MPR) which preserves the geometrical simplicity of active, single sensors and does not compromise operation and location.

1.2 Origins of MPR

For decades sounding has been used in the analysis of planetary atmospheres. Air density and temperature decrease with altitude while molecular spectral emissivity decreases with temperature. Emitting strata interact to produce the spectral radiance upwelling at the top of an atmosphere. This spectrum can be processed to estimate vertical profiles of temperature, density, and pressure [3].

Overhead, nadir-viewing satellites carrying multi-band radiometers probe the Earth's atmosphere in the 60GHz oxygen line and the 4.3μm and 15μm carbon dioxide band. It is important that each species be well mixed as in these cases for altitudes up to about 100km. Carbon dioxide lines are used in probing the atmospheres of Venus and Mars while the 7.7μm line is used for assessing the fairly uniformly mixed methane of Jupiter's atmosphere.

Multi-band data may also be used to extract the "depth" of a bright point source within an atmosphere. Generally, a viewing line of sight (LOS) has both vertical and side-looking components, Figure 1, and a source may be viewed either from above or within the atmosphere. MPR is the application of multi-band processing to passively acquired data from one sensor to the general problem of estimating range along the sensor's LOS to a point source within an atmosphere.

Use of MPR to range to distant TBMs, for which a nearly constant in-band source signature ratio is discussed by Jeffrey et al. [4] for both satellite and aircraft sensors. Earlier passive ranging studies had required either complete knowledge of source spectra or separate rotational lines [5, 6, 7, and 8]. A space-based, nadir-viewing case used many IR radiometer bands and employed neural networks to interpolate altitudes (after "training" based on a limited set of modeled altitudes [9]). MPR is also referred to as "single sensor altitude" method [10].

1.3 Missile Threat Impact

The range calculated from MPR is further combined with measured angular data to derive the 3D boost phase coordinates. Filtering this data to increase accuracy and calculating the BECO (Booster Engine Cut-Off) state vectors allows reconstruction of the missile trajectory using a simple ballistic model. This method allows prediction of

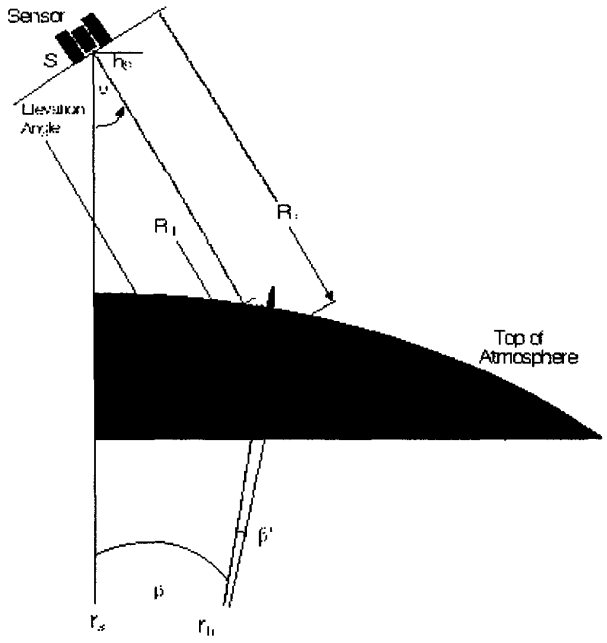

Figure 0 Space sensor viewing geometry with vertical (nadir) and side-looking LOS components [11]

the targets impact point for early warning or communicating cueing volumes to notify defensive radars. By having a small volume to search for targets the radar does not need to be turned on for a long period of time thus reducing the risk of detection and destruction of the radar site.

2. THEORY

2.1 Monocular Passive Ranging

Geometry is central to MPR estimates. A sensor at r_S above the Earth center views a missile along a LOS at range R_1 through the atmosphere at an elevation angle θ, figure 1. From the missile at height h, the sensor is at zenith angle φ (generally is larger than θ due to the Earth's curvature). Atmospheric models define a "top" of the atmosphere at R_T along the LOS.

Absorption occurs in molecular bands along the path R_1-R_T. Atmospheric molecular column density increases in a known way as R_1 increases along the LOS. For a pair of well-chosen bands, the measured band ratio indicates the column density along the LOS. R_1 is found by comparing the two. The CO_2 4.3μm band offers several benefits. It is largely removed from solar clutter, is minimally affected by "weather" (water vapor and dust variations), and is at a strong emission region for TBMs. Jeffrey et al., [4], after

simplifying assumptions, derive the equations for MPR (their equations 7 and 8, respectively). In sum, the known distribution of CO_2 in the atmosphere provides a standard by which distance can be measured.

A non-closed form range derivation illustrates MPR parameter dependencies, Chuang et al. [14]. Source power, S_i, is seen through an atmosphere of transmissivity τ_i in bands i = 1,2. The missile as a "point" source radiates from a pixel of an area that is range squared times instantaneous field of view (IFOV) solid angle $\Delta\omega$ (sr). Behind S_i is a scene background radiance $A_{ib}(R)$ (W/cm^2-sr) from the area $\Delta\omega R^2$. The radiance along the path R is included in A_{ib} in this expression. Scene in-band radiance is A_i (W/cm^2-sr):

$$A_i = \frac{S_i}{\Delta\omega R^2}\tau_i + A_{ib}(R), \quad for \quad i = 1\ \&\ 2 \tag{1}$$

Transmissivity over the path of length R is:

$$\tau_i = e^{-\alpha_0 \int_{R_T}^{R_1} e^{-h/H} dR} \tag{2}$$

Transmissivity is dependent on the altitude of the path R start, R_T, and end, R_1, points and molecular band absorptivity, α_o (km^{-1}). h (km) is the altitude of the air volume dv at range R_1 and H is atmospheric exponential scale height.

Changing variables from R to R' by $R = R_O - R'$, where R_O is the distance from the satellite to the surface of the Earth (see figure 1), τ_i can be written:

$$\tau_i = e^{-\alpha_0 \int_{R'_T}^{R'_1} e^{-\frac{R'\cos\varphi}{H}} dR'} \tag{3}$$

where φ is the local zenith angle along the R path and $h = R\cos\phi$. The integral for τ_i over $R << R_O$ (a near "flat earth" case for which φ is taken to be constant) then becomes:

$$\tau_i = e^{-\frac{\alpha_0 H}{\cos\varphi}\left[e^{-\frac{R'_1\cos\varphi}{H}} - e^{-\frac{R'_T\cos\varphi}{H}}\right]} \tag{4}$$

To obtain a simple form for range a number of assumptions are made. Source radiance is assumed to be approximated by $S_i = \tau_i\, \varepsilon\, Wbb_i(T)$ where $Wbb_i(T)$ is black body radiance in band i at temperature T and ε is source emissivity at band i. The MPR carbon dioxide bands are closely spaced, e.g. 0.2μm bandwidth from 4.3μm to 4.7μm. For present purposes it is assumed that missile exhausts in the 4.6μm spectral region are nearly opaque so that $\varepsilon \approx 1$. If background radiation does not pass through the exhaust and neglecting foreground radiation, then one can take the ratio of the measured radiances in the two bands and reduce it to:

$$\frac{\tau_2}{\tau_1} = e^{-\frac{(\alpha_{02}-\alpha_{01})H}{\cos\varphi} e^{-\frac{R'\cos\varphi}{H}}} \tag{5}$$

Solving for range:

$$R' = -\frac{H}{\cos\varphi}\ln\left[\frac{\cos\varphi}{(\alpha_{02}-\alpha_{01})H}\ln\frac{C}{B}\right]$$
$$\text{where} \quad R = R_0 - R' \tag{6}$$
$$\text{and} \quad h = R'\cos\varphi$$

where the measured and source ratio are: $B = A_2/A_1$ and $C = S_2/S_1$.

FACTORS IN THE SELECTION OF BANDS

The primary issue in the selection of spectral bands for MPR is to minimize the anticipated errors in the estimated range. The most direct way of assessing these errors and thus selecting appropriate bands is to use the expressions developed in the Error Budget section. There are however some graphical techniques that can be used to provide a rapid evaluation of suitable regions for the use of specific band pairs and they are discussed in the following two sections.

BAND RATIO VS. RANGE SPACE

Given that a plot of the band ratios can be or is already available for a specific scenario- which includes sensor height and atmospheric profile- then one can easily evaluate the operational space suitable for MPR with specific band pairs used to generate the plot. In other words, the space defined by elevation angle / range in which the range error would be anticipated to be reasonable. The judgement in this case is to select regions where the slope of the band ratio along a specific line-of-sight is large. Further, if estimates of the fractional error in the band ratio are known then a graphical evaluation of the anticipated range error can be done to further refine the analysis. Among other factors of concern is to avoid MPR "Black-out" regions where the slope of the band ratio is close to zero (the following section provides specific means for identification of the MPR "Black-out" regions). It should be noted that regions in the upper right corner of these plots- typically for upward looking, long range conditions, may have very suitable slopes even though they are positive.

LOCATION OF "BLACK-OUT" REGIONS

The MPR "Black-out" region is defined as those range-line-of-sight regions where the derivative of the band ratio is zero. An analytic means for evaluating these regions can be obtained directly from the expression for the derivation

given in the error budget section. Changing MPR bands can alleviate the 'black-out' effect.

For any given altitude of the target it is assumed that the source band ratio and its derivative with respect to altitude can be generated, perhaps after a curve fit to data computed at a number of discreet altitudes. Then for each altitude one has one equation, in range, R_0, and zenith angle, θ, that comes from setting the slope expression to zero, and a second equation for the altitude in terms of R_0, and θ, that is obtained from the approximate Jeffrey-Draper expression given in Section 2.1.

The given equations can be solved for the following relationship that defines those pairs of range and zenith angles that yield zero slopes for the given altitude.

$$R_0 = \frac{r_e + h_0 - 2K_2}{1 - K_1^2}\left(K_1 + \cos\theta\right) \tag{7}$$

where

$$K_1 = \frac{\exp\left(-\frac{h_t}{H}\right)}{\left(\frac{\partial \frac{S_t}{S_r} / \partial h}{\frac{S_t}{S_r}\frac{1}{(\alpha_{0t} - \alpha_{0r})}}\right)} \tag{8}$$

and $K_2 = h_t - h_0$

2.2 State Vector Estimation

The kalman filter is a data smoothing technique that has one key advantage over most other techniques. The process can begin as soon as the first point has been recorded. This makes kalman filters more applicable to real time situations than most other techniques. There are two different types of kalman filters that are used in this situation. The basic concept of both techniques is to determine the accuracy of a measurement based on previous measurements and a weighting system that takes into account the amount of data that has been processed.

The first kalman filter is the linear kalman filter. This involves three separate filters, one for each ECI coordinate. The result of this filter is a one by three matrix, the three elements being position, velocity and acceleration. The linear kalman filter equation is

$$\hat{x}_k = \phi_k \hat{x}_{k-1} + K_k\left(z_k - H\phi_k \hat{x}_{k-1}\right) \tag{9}$$

$\hat{x}_k$ = filtered values

z_k = measured value

ϕ_k = Fundamental matrix

K_k = Kalman gain matrix

H = Reducing matrix

The fundamental matrix determines the next predicted position value based on the previous filtered position, velocity and acceleration values. The kalman gain matrix weights the measured value based on the amount of data that has been processed, the process noise and the variance matrices. The reducing matrix simply extracts the position value from the filtered matrix.

The second kalman filter is the linearized kalman filter. This involves one filter, a one by seven element matrix. The linearized kalman filter requires a nominal trajectory and thrust to weight information of the missile. It works with differences from the nominal trajectory as opposed to actual trajectory values. The seven elements of this matrix are position and velocity in each coordinate and acceleration. The linearized kalman filter equation is the same as the linear kalman filter equation except the filtered and measured values are replaced by differences between these values and the nominal trajectory.

The linearized kalman filter is much more accurate than the linear kalman filter if the a priori information is accurate, but small errors in the a priori information can cause large errors in the results. For this reason it is preferred to use the linear kalman filter to verify the linearized kalman filter results.

An alternative method that will be pursued in future work is to replace the linear filter with a spline fitting routine. A preliminary look suggests that a spline fit can produce much more accurate results then the linear kalman filter without any a priori knowledge. However, if some target data were available the kalman filter would be much more accurate. A real-time system may include some amalgam of these methods to obtain the best possible estimation of the BECO state vectors.

2.3 Ballistic Coast Model

The flight of a ballistic object can be approximated by a quadratic equation if two pieces of information are known. These are the initial state vectors of the ballistic object and the drag coefficient of the object. The initial state vectors are derived from the pointing information and range information obtained through MPR. These initial state vectors are in terms of position and velocity in ECI coordinates. The drag coefficient can be approximated to an acceptable accuracy for most missiles. With this information the impact point of the missile can be predicted through a step by step iteration.

The iteration used involves propagating the x, y and z position and velocity vectors forward then recalculating the accelerations in all three directions. The formula used for each iteration is the basic formula of motion:

$$x = x_0 + x_0' t_s + \frac{1}{2} a t_s^{\,2} \tag{10}$$

$$x' = x_0' + a t_s \tag{11}$$

x_0 and x'_0 are the position and velocity vectors prior to the iteration and t_s is the sampling time. The acceleration is from gravity and drag. Each component of the gravity vector is determined by multiplying the gravity value at that altitude by each position value and dividing by the distance from the origin, the center of the earth. For example

$$g = -9.78049E^{-3} km/s^2 \tag{12}$$

$$g_h = gR_e^{\,2} / \left(x^2 + y^2 + z^2\right) \tag{13}$$

$$g_x = g_h x / \sqrt{x^2 + y^2 + z^2} \tag{14}$$

Acceleration due to drag is given by

$$a_d = \rho v^2 g / (2\beta) \tag{15}$$

$$a_{dx} = a_d x' / \sqrt{x'^2 + y'^2 + z'^2} \tag{16}$$

ρ is the air density, for altitudes above 9.144 km this is given by

$$\rho = 1.7518 e^{-h/6.7056} \tag{17}$$

below 9.144 km the formula is

$$\rho = 1.225 e^{-h/9.144} \tag{18}$$

The units for ρ are kg/cubic meter. β is the drag coefficient and has units N/square meter. Beta is different for different missiles, but can be approximated to a reasonable accuracy. The value of g used in the drag equation is not an altitude dependant value. The drag coefficient includes the weight of the object in the computation, multiplication by gravity cancels this out, leaving just mass which is needed to give us a drag acceleration as opposed to a drag force.

This iteration is continued until the altitude of the object is zero. The step size is variable, but steps smaller than 1 second do not seem to make any appreciable difference.

3. IMPLEMENTATION

3.2 Storage Requirements

The storage requirements are driven by the need to store sufficient number of atmospheric transmission values to cover the anticipated measurement scenario extremes. The following estimate is based on currently understood variability of MPR range estimates.

1. Sensor altitude – The measured sensor altitude is quantized to a variable step that is approximately 10% of the actual altitude. Therefore, the number of discrete altitudes that are needed for the atmospheric database are typically less then 10.
2. LOS angles – typically 9 degrees at a 0.5 degree resolution. However, as the LOS approaches the limb the resolution must be increased to 0.1 degrees since atmospheric transmission can vary rapidly at those angle – net of 50
3. Slant range – currently 100 values over the anticipated mission dictated ranges.
4. Spectral "bins" – The atmosphere is run in 5 wavenumber units. Within are current spectral region of interest this equates to 601 spectral bins. This region is currently large because the out of band rejection must be accounted for. If the spectral region could be capped the actual storage could be reduced by a factor of six.

The total memory required might then be as large as

10*100*50*601*2 = 57 Mbytes (19)

Assuming 2 bytes per transmission value. With a simple compression routine this database could be reduced by a quarter with minimal loss in data access speed. In addition, this database is what would be required for any scenario within the possible look directions of the sensor. This could be greatly reduced if any operational or mission requirements were imposed upon it.

3.3 Real-time MPR

The current algorithm is near real-time, but only on a data rate of 1 Hz. This is adequate for testing purposes but for an operational system a much higher data rate would be desired. Additionally, for flexibility, several source signatures in addition to a generic black body signature may want to be run in parallel. This method could prove valuable to other missile ID routines that could use range as a measure of interest.

The ballistic coast model is not computationally intensive and already runs in real-time. The intensive parts of MPR lie in the calculation of the atmosphere and the interpolation of the target signature intensities (from a database) to desired points along the line of sight. The purpose of this section is to provide estimates of the processing and memory requirements for the basic MPR algorithm used in a serial processor in a real time mode. It will be assumed that the target intensity determination in both MPR spectral bands has already been accomplished via other processors, as well as the determination of the line-of-sight direction. Specifically that at each frame time the target apparent intensity in both bands together with the Los elevation angle of the target relative to local horizontal at the sensor, and the sensor altitude, is provided to the MPR processor together with UTC or TALO.

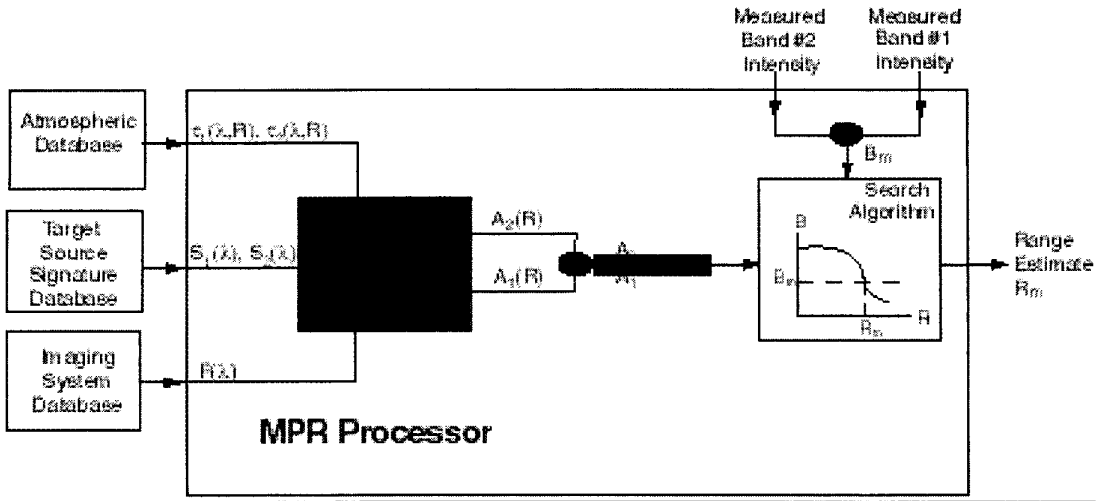

Figure 2 MPR Data Processing System

The purpose of the MPR processor is to compute the corresponding slant range between the sensor and the target. The processor functional calculations are shown schematically in Figure 1(???). The two measured band intensities are ratioed and then compared to modeled band ratios computed at different slant ranges until a sufficiently accurate match is obtained. The modeled band ratios are obtained by spectrally summing the product of the target source signatures, the atmospheric transmission along the slant path, and the filter response of the imaging system. The atmospheric transmission is obtained from an interpolated look up into an atmospheric data base computed offline using such codes as Modtran. The interpolation covers elevation angle, sensor altitude and target range. The source signature, which depends on altitude, is likewise interpolated from a second database.

The spectral region used in the band model depends upon the spectral response in the tails of the band filters that are provided spectrally in the imaging system database. Using a spectral resolution of 5cm-1 typical to Modtran, then there will be 101 spectral samples if the band pass used is 4-5 microns and 601 if it is 2-5 microns.

We will enumerate the number of floating point operations for the processor with the following assumptions;

- The required interpolation in atmospheric transmission and source signature will require one add and one multiply respectively for each spectral bin
- The iterative procedure to determine range is accomplished by successive range calculations with the range interval bracketing and the measured band ratio reduced by a factor of two at each step. This leads to a percentage range accuracy of less than $1/2^{n-2}$. This would require 5 iterations to achieve a range accuracy of 10% and 7 iterations to achieve 3% and 9 iterations to achieve 1% accuracy.
- The add and multiply operations are assumed the same in the enumeration.

Assuming there are N spectral bins then there are 4N FLOPS for the Atmospheric and Source signature interpolations for each range calculation. This is followed by 3N multiplies and N adds to obtain a total of 8N FLOPS for each of two bands or a total of 16N FLOPS for each range calculation. We have ignored operations that need not be repeated for each spectral bin.

The total MPR operations to achieve a range estimate with an accuracy of P percent is then

$$n * 16N$$

where

$$\mathrm{Int}(100/2^{n-2}) = P$$

Finally if the MPR processor frame time is F frames per second the total operations is

Floating Point Operations per second $= F * n * 16\ N.$

For example with F= 30Hz, N= 101 spectral bins (4-5 band), and n=9 for 1% accuracy we require 436,320 FLOPS, and 2,596,320 FLOPS if the spectral band is increased to 2-5 microns.

4. ERROR BUDGET

4.1 MPR Error Budget

There are two major differences between this model and previously developed ones[1], and these are the use of a

[1] CK. Chuang, M.Wohlers, J.S.Draper,"MPR Error Budget Analysis for Air or Space Borne Missile

round earth model, and the allowance for altitude variations in the target plume signature. The first modification is accomplished using a second order correction for the earth curvature that was used in the basic Jeffery-Draper model[2]. The second involves a first order correction to the Source Band Ratio and a direct formulation of the MPR processing algorithm.

These modifications are critical for long range scenarios where the earth's curvature introduces range errors, and the variation of the source signatures can lead to multiple solutions for range in the basic MPR algorithm, and more importantly large errors in range estimation in the near horizontal viewing scenario.

This budget describes the modified model, presents analytic formulas for range error due to various sources, and discusses procedures for the selection of spectral bands that minimize the range errors in given scenarios.

IMPROVED MPR PROCESSING MODEL

The basic MPR algorithm is a model based approach to estimating the range to a target using ratios of measurements in two spectral bands and comparison to modeled values obtained for the same scenario parameters. In its most accurate form it uses detailed models of the atmospheric attenuation in the two spectral bands as is available in codes such as MODTRAN. However, in order to obtain system level estimates of its performance, and for initial selection of spectral bands, it is useful to have first order analytic models of performance, including error bars for various random effects such as sensor noise, data processing residuals, atmospheric variations, etc. The primary purpose or this note is to expand on previously developed models in order to provide a means for predicting various trends, such as the effects of altitude variation of target source signature that was not included in previous treatments.

BASIC MPR ALGORITHM

The basic MPR algorithm is shown schematically in Figure 2.1-1. The basis for the calculation is a model-based evaluation of the ratio of two spectral band outputs, denoted B(R). This is computed by evaluating the response of the detector to a given source signature as it is propagated through the atmosphere along a given line of sight. The measurement model shown in the figure is an integration of the product of the Source signature S(λ), the atmospheric transmission τ(λ), and the sensor response F(λ). The source model generally is obtained from detailed plume signature codes at a series of altitudes and then interpolated to various altitudes as needed. The atmospheric transmission can be obtained, as noted previously, from detailed models such as MODTRAN, or as discussed in Section 2.2 approximately using simpler Beers law models. Finally, the sensor model can take on various levels of detail but in the simplest form it is a model of the filter function corresponding to each band. In simplest form the Measurement model is the product of the integrated source intensity over the spectral band times the average atmospheric transmission over the band. The model described in this paper is of that form.

The final determination of the range estimate involves a comparison of the actual measured band ratio, B_m, to the results of the evaluation of the model in order to find the closest fit. The error in the evaluation of range due to fractional errors in the measured band ratio can be written as

$$RangeError = \frac{\frac{\Delta MeasuredB}{B}}{\left|\frac{\left(\frac{\partial B}{\partial R}\right)}{B}\right|} \qquad (20)$$

Thus the larger the magnitude of the fractional slope of B Vs range, the smaller the range error. Note that when the slope is near zero one has very large error and the MPR algorithm ceases to function – a region we denote as MPR "Black-out".

ROUND EARTH ATMOSPHERIC MODEL

The simpler atmospheric transmission model advanced by Jeffery-Draper[3] assumes that the transmission follows Beers Law, i.e. it is an exponential function of the atmospheric extinction coefficient, κ_{ext}, along the sensor line-of-sight to the target. Moreover, that the extinction coefficient dependence with altitude is also exponential with a scale height H. If we take a line of sight at a fixed zenith angle θ, as measured at the sensor, then the transmission is evaluated from the integral expression

$$\tau = \exp\left(-\alpha_0 \int_0^{R_0} \exp\left(\frac{-h(r)}{H}\right) dr\right) \qquad (21)$$

where α_0 is the extinction coefficient at ground level, and h(r) is the altitude at a range ,r, along the line of sight.

The altitude h (r) can be obtained from the spherical earth model and repeated application of the Law-of-Sin's as

$$h(r) = \sqrt{(r_e + h_0)^2 - 2r\cos\theta(r_e + h_0) + r^2} - r_e \qquad (22)$$

Surveillance" IRIS MD-SEA Symposium,January 1999

[2] Jeffrey,W, J.s.Draper, R.Gobel,"Monocular Passive Ranging",IRIS TBD Symposium, January 1994

[3] Jeffrey,Draper,et al IRIS 1994

where r_e is the radius of the earth and h_0 is the sensor altitude. This expression can be simplified, as noted in Jeffry-Draper, by expanding the square root in a power series up to order two. The resulting expression for h is then

$$h(r) = h_0 - r\cos\theta + \frac{1}{2}\frac{r^2\sin^2\theta}{r_e + h_0} \tag{23}$$

which can be substituted into the Beers Law model.

ALTITUDE DEPENDENT SOURCE RATIO

An expression for the band ratio B from two spectral bands can be obtained using the round earth model developed in Section 2.2 as

$$B = \frac{S_T}{S_R}\exp\{-(\alpha_{0t} - \alpha_{0r})\int_0^{R_0}\exp\left[-\frac{\left(h_0 - r\cos\theta + \frac{1}{2}\frac{r^2\sin^2\theta}{r_e + h_0}\right)}{H}\right]\partial r\} \tag{24}$$

where

S_T and S_R are the source intensities in each band

α_{0t} and α_{0r} are the average sea level extinction coefficients in each band

h_o is the sensor altitude

H is the atmospheric species scale height

r_e is the radius of the earth

θ is the zenith viewing angle to the target, and

R_0 is the range to the target.

The error in the evaluation of range due to fractional errors in the measured band ratio can then be written as

$$RangeError = \frac{\frac{\Delta MeasuredB}{B}}{\left|\frac{\left(\frac{\partial B}{\partial R}\right)}{B}\right|} \tag{25}$$

where

$$\frac{\left(\frac{\partial B}{\partial R}\right)}{B} = \frac{\left[\frac{\partial\frac{S_T}{S_R}}{\partial h}\right]}{\frac{S_T}{S_R}}(h'(r)) - (\alpha_{0t} - \alpha_{0r})\exp\left(-\frac{h(r)}{H}\right)\Bigg] \tag{26}$$

h(r) is the altitude of the target and h'(r) is given by

$$h'(r) = \left[\left(-\cos\theta + \frac{R_0\sin^2\theta}{r_e + h_0}\right)\right] \tag{27}$$

It is clear from this expression that altitude dependent source band ratios directly influence the resulting range estimation errors, in particular they can cause unbounded error at range / line-of-sight look angle pairs for which the previous expression is zero. It is also clear from the expression that this can not occur if the source ratio is constant.

The general form of the plot of band ratio versus range can also be determined from the last expression. For example, assuming that $\alpha_{0t}>\alpha_{0r}$ and that the source band ratio increases with altitude- a typical situation using bands located on the Red wing of the CO_2 band- then for short ranges and negative zenith angles the band ratios are a decreasing function of range. That trend continues until the slope goes to zero and then reverses to an upward trend at longer ratios. The same general result holds for positive zenith angles (looking upward) but the transition to upward trend occurs at shorter ranges.

RANGE ERRORS FROM SPECIFIC SOURCES

Expressions for the random MPR range error can be obtained from the expressions generated in previous section. If we consider five such sources, i.e. Sensor noise, Data Processing errors, Source variations, Atmospheric variations, and line-of-sight variation then assuming that they are all uncorrelated random effects we have

$$\sigma_R = \left|\frac{1}{\frac{\partial B}{\partial R}/B}\right|\sqrt{\left(\frac{\sigma_{BS}}{B}\right)^2 + \left(\frac{\sigma_{BDP}}{B}\right)^2 + \left(\frac{\sigma_{BSOU}}{B}\right)^2 + \left(\frac{\sigma_{BA}}{B}\right)^2 + \left(\frac{\sigma_{BLOS}}{B}\right)^2} \tag{28}$$

1) Sensor noise

$$\frac{\sigma_{BS}}{B} = \sqrt{\left(\frac{N_t}{A_t}\right)^2 + \left(\frac{N_r}{A_r}\right)^2} \tag{29}$$

where N_t and N_r are the RMS values of the measurement errors in each band, and A_t, A_r are the corresponding measured band values. Note that the measured sensor signal can be determined as

2) Data processing error

$$\frac{\sigma_{BDP}}{B} = \left[\sqrt{2}\frac{\sigma_{DP}}{A}\right] \tag{30}$$

3) Source Uncertainty

$$\frac{\sigma_{BSOU}}{B} = \frac{\sigma_C}{\overline{C}} \tag{31}$$

where

$$\left(\frac{\sigma_C}{\overline{C}}\right)^2 = \left(\frac{\sigma_{S_t}}{S_t}\right)^2 + \left(\frac{\sigma_{S_r}}{S_r}\right)^2 - 2r\frac{\sigma_{S_t}}{S_t}\frac{\sigma_{S_r}}{S_r}$$

with "r" the correlation coefficient of noise in S_t and S_r

4) Atmospheric Variation

$$\frac{\sigma_{BA}}{B} = \sigma_{(\sigma_{0t}-\sigma_{0r})}\int_0^{R_0}\left[\exp\left(-\frac{\left(h_0 - r\cos\theta + \frac{1}{2}\frac{r^2\sin^2\theta}{r_e + h_0}\right)}{H}\right)\right]dr \tag{32}$$

5) Line of sight uncertainty

$$\frac{\sigma_{Blos}}{B} = \sigma_{los}\frac{(\sigma_{0t}-\sigma_{0r})}{H}\int_0^{R_0}\exp\left(-\frac{(h(r))}{H}\right)\left[r\sin\theta + \frac{r^2\sin\theta\cos\theta}{r_e + h_0}\right]\partial r \tag{33}$$

4.2 Ballistic Coast Error Budget

This paper presents a novel technique used to perform missile flight analysis with data obtained during the powered flight portion of an event. The proposed technique is distinguished by the fact that a 3-dimensional missile track can be obtained using data derived from a single passive collection platform. The data sets consist of two metric, orthogonal, angular data sets, and range data derived from the spectral content of the data. The three data sets are referred to as Right Ascension (RA), Declination (DEC), and Slant Range (SR). KTAADN"s Monocular Passive Ranging (MPR) technique is used to derive the Slant Range data set. The MPR technique has is discussed in section 2.

The data sets are collected only during the powered flight portion of the event. However, the RV and/or tank impact location can be estimated by propagating the vehicle state vector forward from the booster engine cut-off (BECO) point. Two techniques have been used to "fit" the data sets and derive the missile flight parameters during powered flight. The two techniques are a Kalman Filter estimation technique, and an analytic technique.

Using either flight analysis technique, the accuracy of the trajectory parameters derived during powered flight is a function of the quality of the data sets. The process of estimating impact location based upon powered flight data sets consists of five basic steps:

1) Acquire RA and DEC data sets
2) Calculate Slant Range (SR) data set via Monocular Passive Ranging (MPR) technique
3) Using either the Kalman Filter technique or the analytic technique, estimate the powered flight portion of the vehicle position and velocity histories using RA, DEC, and SR data sets
4) Hand-off best estimate of position and velocity state vector from end of powered flight mode to start of ballistic/re-entry mode
5) Propagate vehicle state vector from BECO to impact

Since neither the data sets nor the flight analysis techniques are perfect, errors will result in the position and velocity components at the end of the missile burn period (BECO). An error analysis has been performed to quantize the variations at the impact location based upon errors in the state vector at BECO. The required accuracy of the data sets can be established from results of the error analysis. Errors in the position and velocity vectors at BECO are functions of the error levels in the data sets. Results from the error analysis exercise will show how errors in the state vector at BECO translate to variations in the impact location relative to the true impact location. Consequently, by knowing the maximum allowable impact location variation, the maximum allowable error levels in the data sets can be established.

To perform the error analysis, a simulated trajectory was calculated. Following are key parameters from the simulated trajectory:

Launch Location	
Latitude	39.0°
Longitude	271.0°
Flight Heading	245.2°
Guidance Scheme	Gravity Turn
BECO	
Time	80 sec past launch
Speed	2463 m/sec
Down range	34.5 km
Apogee	
Time	299 sec past launch

Altitude	272.64 km
Down range	340.9 km
Impact	
Time	547.4 sec past launch
Location	
Latitude	36.336°
Longitude	263.951°
Total Down Range Distance	688.3 km
RV Ballistic Coefficient	14,000 kg/m^2

IMPACT ERRORS RESULTING FROM STATE VECTOR ERRORS AT BECO

To calculate impact location variations based upon errors at BECO, errors in up, down, and cross range position and velocity were added to the nominal state vector at BECO (80 seconds past launch). The resulting state vectors were then flown to impact using a 4th order integration scheme, a standard atmospheric model, and a 4th order earth model. The ballistic coefficient of 14,000 kg/m^2 used to generate the simulated trajectory was also used to propagate the state vectors from BECO to impact. Impact variations were calculated to determine the sensitivity of impact location to errors in position and velocity at BECO.

Position errors in down range and cross range tend to translate one-for-one to the impact location. That is, an error of 100 meters in down range position at BECO results in a 100 meter down range error at impact. However, variations in the impact location tend to be more sensitive to errors in the velocity vector at BECO than to position errors at BECO.

To calculate impact location variations due to errors in the velocity vector, velocity errors were introduced in the plus and minus up range, down range, and cross range directions at BECO. The magnitude of the errors used in this study are 1%, 5%, and 10% of the velocity magnitude at BECO (2463 m/sec). Thus, the error levels are +/-25 m/sec, +/-125 m/sec, and +/-250 m/sec. Figure 1.1 illustrates the resulting impact locations due to the velocity errors at BECO.

It is also important to note that combinations of errors in down range and cross range will produce an impact location variation that is very nearly a linear combination of the two individual variations. Also, variations in impact location due to errors in position and velocity are additive.

The error analysis results presented in this paper are for the simulated trajectory and the state vector error levels described above. A more comprehensive error analysis can be performed by including trajectories with different flight characteristics, and by varying additional model parameters.

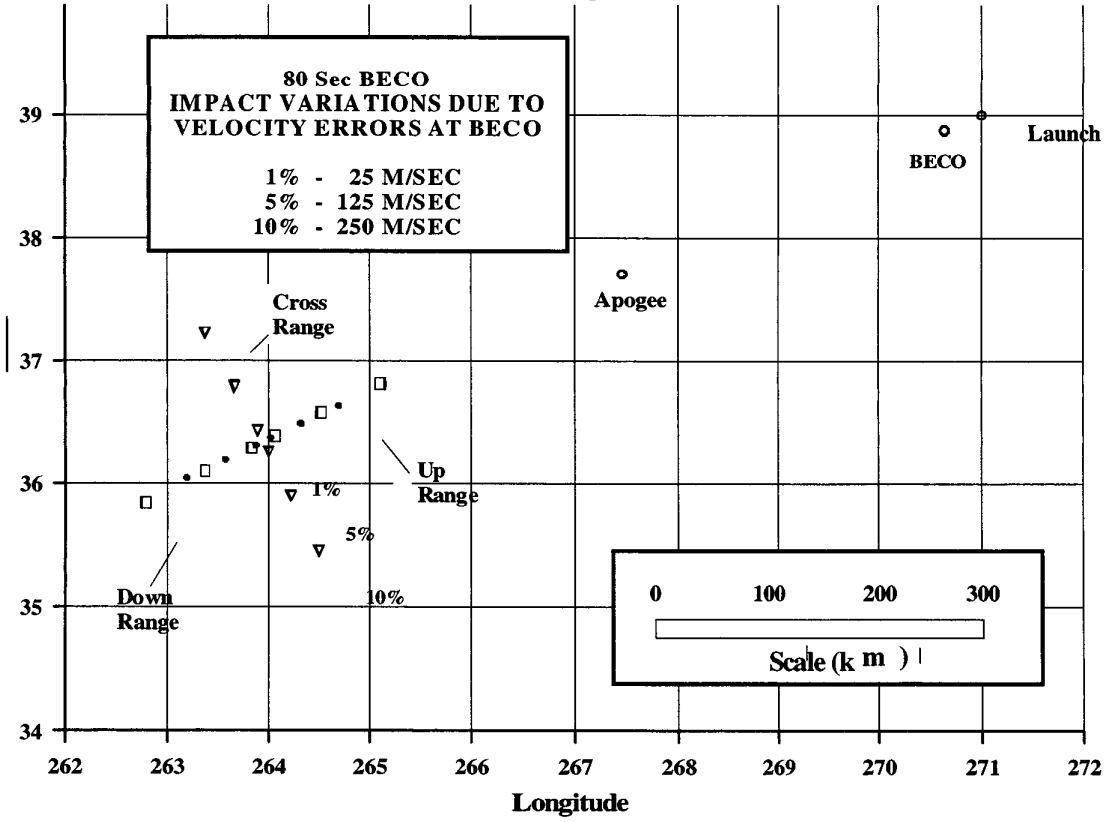

Figure 3 Ballistic Coast Errors

5. CONCLUSION

Missile trajectory tracking and impact prediction by passive means will become an increasingly important in the severe ARM environment of future battlefields. The MPR model for passively reporting missile flight and predicting impact is under study. Validation of MPR ranges against distant missiles is being pursued. Three analyses support the value of MPR ranges (ARGUS data [4], satellite data [20], and ARES data [21]). Verification field programs are under review [22]. Also ongoing are examinations of potential new defense approaches made possible by MPR systems such as boost phase intercepts [23, 24].

For TBM tracking missions the potential value of MPR impact prediction is that it uses a single sensor, is fast and passive. TBM impact predictions are quite "perishable" and require responsive transmission over available narrow band comm links to military users. The MPR model offers a technologically practical to provide such responsive impact predictions.

Success of MPR applications may bring a number of benefits. TMD impact predictions could be rapidly and covertly reported. Cueing of major ground based (GBR) and airborne radars might proceed using MPR-based data acquired both before and at ECO. Forward located MPR sensor and processing packages, when deployed in large numbers, could send back expected tracks well before the TBM warheads break radar horizons. For both TMD impact prediction and GBR cueing, only one sensor is needed. This means that impact predictions or radar cues can be formulated rapidly at the sensor and be sent directly to defenders.

MPR employs well-understood electro-optical sensors that are small, light, frugal in the use of power, and inexpensive. Satellite constellations might be considerably reduced and simplified. Overall, as battlefields become more dangerous for radar a family of covert, high-speed reporting MPR-based ranging systems may emerge to complement and support radar.

6. GLOSSARY

A	reference cross-section
A_D	drag
A_E	engine exit area
A_i	apparent radiance of plume, in W/cm^2-sr
ΔA_i	incremental in-band radiance, the AC term of A_i
α_o	atmospheric extinction coefficient at h = 0, in km^{-1}
B_{ij}	in-band radiance ratio of band i and band j
ΔB_{ij}	incremental in-band ratio
BS	background subtraction residual
C_{ij}	in-band source ratio between band I and band j
C_D	drag coefficient
D	dark current
$\Delta\alpha_o$	α_o difference between band i and band j
ECO	engine cut-off
EEP	error ellipse of probability
$f(,,)$	range equation function
F	foreground noise
FOV	field of view
GBR	ground based radar
h	target altitude, in km
h_s	sensor altitude, in km
H	air density scale height, in km
$IFOV$	instantaneous FOV
I_{SP}	propellant specific impulse
K	gain factor for non-uniform correction
LOS	line of sight
M	stage initial mass
$\dot{m}$	mass flow rate
MPR	monocular passive ranging
φ	target zenith angle between LOS and local normal
R_t	range from sensor to model "top" of the atmosphere
R_o	LOS ground intercepting range, in km
R_l	target range from sensor, in km
R'	target to ground range, in km
$R = R_l - R_t$	slant range in atmosphere, in km
$\sigma^2_x = E[\varepsilon^2_x]$	variance of e
TBM	theater ballistic missile
τ_l	LOS transmission in band I
t_k	TBM kickover time at boost phase
θ	sensor look angle between LOS and local vertical
V_A	flight speed

7. REFERENCES

[1] Anon., "Air-Delivered Missiles in Desert Storm," http://pw1.netcom.com/~chadeast/missiles/missile.html, November 10, 1998.

[2] Anon., "China Shows New AWACS-Killer Missile," *Jane's News Briefs*, September 15, 1998.

[3] C. Elachi, *Introduction to the Physics and Techniques of Remote Sensing*, Wiley & Sons, 1987.

[4] W. Jeffrey, J.S. Draper, R. Gobel, "Monocular Passive Ranging," *IRIS Targets, Backgrounds and Discrimination Conference*, Monterey CA, February 1-3, 1994.

[5] J.B. Restorff, "Passive Ranging Using Multi-Color Infrared Detectors," *NSWC-TR-81-401*, 1981.

[6] N.K. Leonpacher, "Passive Infrared Imaging," *AFIT/GEP/PH/83D-5*, MS Thesis Air Force Institute of Technology, WPAFB OH, 1984.

[7] P.L. Roney, M. Gauvin, "Development of the Theory of Passive Ranging (U)," *DREV R-4386/86*, 1986 (Secret).

[8] D.J. Gregoris, "Passive Ranging Technique for Infrared

Search and Track (IRST) Systems," US Patent No. 5,282,013, Issued January 26, 1994.

[9] Draper, J. S., "Feasibility of Single Sensor Altitude", Presentation to USAF/NAIC User's Meeting, PAFB FL, July 21, 1993.

[10] H. E. Evans, B. A. Hibbeln, "The Theory of Single Sensor Altitude Determination", *Proceedings 17th IEEE Aerospace Applications Conference*, vol. 3, pp 53-66, IEEE Service Center, Piscataway, NJ, February 1996.

[11] S.E Perlman, C.K Chuang, J.S. Draper, E.M. Powers, D.S. Frankel, H. Evans, L. Lillard, B.A. Hibbeln, "Passive Ranging for Detection, Identification, Tracking and Launch Location of Boost Phase TBMs," *IRIS Passive Sensors Conference*, Monterey CA, March 12-13, 1996.

[12] S.E. Perlman, J.S. Draper, C.K. Chuang, E.M. Powers, H.E. Evans, L. Lillard, T. Hoeger, "Launch Site and Impact Point Prediction and Defensive Missile Cueing Using a Single Passive 3-D IR Sensor with Arbitrary Filter Shapes, Look-Down Angles and Target Identification (U)," *IRIS Passive Sensor Conference,* Tucson AZ, Mar 4-6, 1997 (S).

[13] L. Lillard, private communication, September, 1997.

[14] C.K. Chuang, J.S. Draper, S.E. Perlman, E.M. Powers, D.S. Frankel, H.E. Evans, "An Autonomous Approach Toward Monocular Passive Ranging," *IRIS Targets, Backgrounds and Discrimination Conference*, Monterey CA, February 4-7, 1997.

[15] C.K. Chuang, M.R. Wohlers, M.A. Hanson, J.S. Draper, H. Evans, R. Cody, D. Sene, "MPR Error Budget Analysis for Air or Space-borne Missile Surveillance," *IRIS MD-SEA*, Monterey CA, January 1999.

[16] M.R. Wohlers, "Monocular Passive Ranging (MPR) Error Caused by Atmospheric Variability", KI-R-98-020, KTAADN, INC., Newton, MA, October 27, 1998.

[17] Anon, Milestone Data Base, USAF/NAIC 1998, (S).

[18] "Department of Defense World Geodetic System 1984," Technical Report #8350.2, Washington, DC, U.S. Naval Observatory, 1987.

[19] S.E Perlman, C.K Chuang, J.S. Draper, E.M. Powers, D.S. Frankel, H. Evans, L. Lillard, Capt D. Sene, Tracking, Launch Site Estimation and Impact Prediction of TBMs Using a 3-D Passive, Satellite-Borne IR Sensor," *National Fire Control Symposium,* Eglin AFB, Aug 1996.

[20] D.S. Frankel, C.K. Chuang, J.S. Draper, D. Adams, S. Barrett, "Target Trajectory Estimation: Monocular Passive Ranging by a Single Sensor Compared to Stereo Viewing (U)," *IRIS Targets, Backgrounds and Discrimination Conference*, Monterey CA, February 4-7, 1997 (S).

[21] M.R. Wohlers, private communication, November, 1998.

[22] D.L McKay, M.R. Wohlers, J.S. Draper, "MPR Airborne Validation," KTAADN briefing to NAIC, WPAFB, OH, November 12, 1998.

[23] J. Draper, P. Zarchan, W. Frederick, D. McKay, "Interceptor Propellant Use vs. Range Accuracy," *7th Annual AIAA/BMDO Technology Readiness Conference and Exhibit,* Colorado Springs, CO, August, 1998.

[24] J.S. Draper, W. Frederick, W. Smith, "Assessment of MPR for UAV/KKV BPI," *6th Annual AIAA/BMDO Technology Readiness Conference and Exhibit,* San Diego, CA, August 1997.

VIII. BIOGRAPHIES

Matthew. Hanson *is responsible for writing and developing code for signal and image processing applications such as Monocular Passive Ranging (MPR) or display projects. Currently Mr. Hanson is working on an innovative algorithm, BIGBIRD, which processes from a single sensor missile tracker. BIGBIRD performs trajectory estimation on a boosting missile and predicts its launch point, impact point and cueing volumes. He is managing the project in addition to developing code that supports passive ranging output, trajectory estimation and impact prediction. Some of the elements include an examination of a Trajectory Matching Code, a parametric study of Kalman filtering accuracy, a basic code for simple decoupled Kalman filter built into BIGBIRD software. He is also generating the graphical user interface for PRIMER, KTAADN's early ID software which provides a rapid scheme for analyzing sensor data and offers accurate missile and bomb identification. Mr. Hanson received his BS in Imaging and Photographic Technology at the Rochester Institute of Technology in 1995.*

Kevin Tibbetts *has been with KTAADN for approximately one year as an engineer. A large portion of his effort has involved writing and developing code for IMPRESS, KTAADN 's Monocular Passive Ranging (MPR) software written in IDL code and PRIMER, an early ID software which provides a rapid scheme for analyzing sensor data and offers accurate missile and bomb identification. In addition, Mr. Tibbetts is processing and analyzing the intensity data for Low Intensity Conflict analysis, a project*

reporting, tracking and analyzing specific ordnance event collects from a new sensor. Mr. Tibbetts received his BS in Engineering Physics in May of 1998 from the University of Maine. While attending the University of Maine he worked at the Laboratory for Surface Science and Technology on campus as an Engineer Assistant.

***Ronald Wohlers**, an engineer experienced in infrared systems with a concentration in the Department of Defense arena, joined KTAADN as Chief Engineer on our AST and HALO/Monocular Passive Ranging (MPR) projects. Recent accomplishments include the analysis of the errors in the MPR range estimates, the performance of MPR using ARES data collected during the Willow Dune experiment, and the planning and data analysis of HALO/IRIS data collected at the SFX and CODA missions. He is responsible for IR phenomenology and sensor system performance as it relates to Monocular Passive Ranging technology. This includes all phases of sensor system design, integration aboard the HALO, and pre- and post mission analysis. Mr. Wohlers received his BEE, Summa Cum Laude, from Polytechnic Institute of Brooklyn in 1955 and his MS from the University of Maryland, (Electrical Engineering) in 1959.*

***Jack D. Hart** - After receiving his degree in Aerospace Engineering from the University of Texas at Austin, Mr. Hart worked for seven years at the Central Intelligence Agency in Washington, D.C. While at the CIA, Mr. Hart developed flight analysis computer code, and performed extensive analysis on the flight performance of missile systems. Mr. Hart left the CIA to work at Radian Corporation where he spent 17 years serving in Radian's Special Projects Department. From 1986 to 1993, Mr. Hart was the Special Projects Department Head. While at Radian, Mr. Hart continued to serve the DoD community by further developing numerous flight analysis computer programs, many of which are still in use today. Mr. Hart also analyzed and documented more than 100 missile events. Many of his flight analysis reports have received international distribution. Also while at Radian, Mr. Hart provided flight analysis support to the U.S. Army, U.S. Air Force, Britains' Ministry of Defence, and other agencies. He has also developed flight analysis tutorials and provided training to U.S. Army, U.S. Air Force, and Royal Air Force personnel. After leaving Radian, Mr. Hart served as the Technical Manager at The University of Texas at Austin Center for Space Research. Since leaving the Center for Space Research, Mr. Hart has acted in a consulting capacity, primarily as a technical contributor on DoD projects.*